Full Tokamak Discharge Simulation for ITER

S.H. Kim[1], J.-F. Artaud[1], V. Basiuk[1], V. Dokuka[2], G.T. Hoang[1], F. Imbeaux[1], R.R. Khayrutdinov[2], J.B. Lister[3], V.E. Lukash[4]

[1]CEA, IRFM, F-13108 St Paul-lez-Durance, France
[2]TRINITI, Troitsk, Moscow Region, 142190, Russia
[3]EPFL, CRPP, Association Euratom-Confédération Suisse, CH-1015 Lausanne, Switzerland
[4]Institute of Nuclear Fusion, RRC Kurchatov Institute, Moscow, 123182, Russia

Email contact of main author: sun-hee.kim@cea.fr

Abstract. A full tokamak discharge simulator has been developed by combining CRONOS and DINA-CH. The two codes have been coupled in a modular way using an explicit data exchange scheme and used to study the proposed ITER operation scenarios. Firstly, the inductive 15MA ITER H-mode scenario has been simulated as a demonstration of the capability of the simulator, as well as a design study in itself. The engineering and operational constraints are taken into account for whole operation phases including the plasma current ramp-up, flat-top and ramp-down. The poloidal field (PF) coil current limit, poloidal flux consumption, plasma shape evolution and vertical instability associated with a high internal inductance were investigated to assess the feasibility of the scenario. Secondly, lower hybrid (LH) assisted plasma current ramp-up has been studied. Application of the LH during the current ramp-up was effective in lowering the internal inductance to be favourable for vertical stabilization of the plasma and also in reducing the poloidal flux consumption. A slightly reversed or flat target safety factor profile required to operating ITER plasmas in advanced tokamak regimes was achieved avoiding the onset of sawteeth during the current ramp-up phase. Lastly, the ITER hybrid mode operation scenario has been studied aiming at achieving a stationary flat safety factor profile at the beginning of the current flat-top phase. The plasma current ramp-up scenario is generated by tailoring the initial part of the inductive 15MA H-mode ITER pulse and the effect of different heating and current drive schemes on the evolution of the safety factor profile has been investigated. Application of near on-axis electron cyclotron current drive (ECCD) appears to be effective in modifying the safety factor profile compared with far off-axis lower hybrid current drive (LHCD), at least on short time scales.

1. Introduction

Understanding non-linearly coupled effects between plasma transport and free-boundary equilibrium evolution is essential for investigating the detailed evolution of a tokamak discharge. All the major events observed in a tokamak discharge, such as the plasma current ramp-up and ramp-down, energy confinement mode transitions, MHD instabilities, application of additional plasma heating and current drive (H&CD), minor and major disruptions, and evolution of internal transport barriers, are strongly subject to non-linearly coupled effects. Besides, the engineering constraints in operating the tokamak, such as the poloidal field (PF) coil current and force limits, can add additional non-linearities to the plasma control system. Therefore, all the related physics and engineering constraints have to be self-consistently included into a tokamak discharge simulation.

We have achieved this full tokamak discharge simulation capability by combining a non-linear free-boundary plasma equilibrium evolution code, DINA-CH [1-2], and an advanced transport modelling code, CRONOS [3], in a modular way (see FIG. 1) . In this combined tokamak discharge simulator, DINA-CH self-consistently calculates the non-linear evolution of the free-boundary plasma equilibrium with the plasma current diffusion, in response to both controlled PF coil currents and inductively driven currents in the surrounding conducting systems. CRONOS provides the evolution of the kinetic plasma profiles by self-consistently solving heat and particle transport with source profiles. The free-boundary plasma equilibrium provided by DINA-CH is directly used for CRONOS transport and source calculations. The plasma and source profiles provided by CRONOS are directly used for DINA-CH in calculating the free-boundary equilibrium and current diffusion. All the exchanged data between DINA-CH and CRONOS are passed as SIMULINK variables explicitly in time with a sufficiently small time-step (~1ms) to ensure the convergence. Although this explicit data exchange scheme slightly deteriorates the consistency of the coupled physics, compared with a fully implicit scheme solving a complete set of coupled transport equations, this was an inevitable choice to guarantee computational performance and reliability of the combined tokamak discharge simulator. With this code coupling scheme, the two codes are combined maintaining their original code structures.

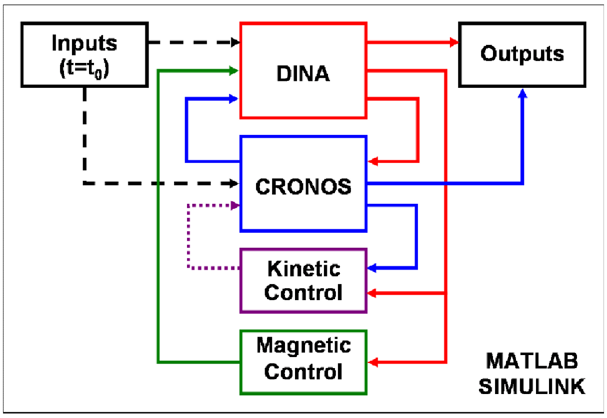

FIG. 1. Code coupling scheme used for the combined DINA-CH and CRONOS tokamak discharge simulator. Controlling the kinetic profiles is work in progress (dotted line). Reprinted from Figure 1 of [5].

In this paper, we summarize our recent research activities [4-6] on the full tokamak discharge simulation for ITER using the combined DINA-CH/CRONOS simulator. Section 2 presents a full tokamak discharge simulation of the inductive 15MA H-mode ITER scenario [4-5], as a demonstration of the capability of the combined tokamak discharge simulator, as well as being a design study in itself. Section 3 discusses lower hybrid (LH) assisted plasma current ramp-up [6], focusing on the capability of saving flux consumption. Section 4 introduces a study on the ITER hybrid mode operation [5]. Conclusions are presented in section 5.

2. Full Tokamak Discharge Simulation of the Inductive 15MA H-mode ITER Scenario

The inductive 15MA H-mode ITER scenario [7] has been successfully simulated [4-5]. This operation scenario (see FIG. 2) is designed to ramp the plasma current up to 15MA and to be able to achieve about 400s of plasma burn in ELMy H-mode conditions. In this inductive scenario, the possible length of the current flat-top phase is generally limited by the consumption of the poloidal flux during the current ramp-up phase. At the end of the current flat-top phase, the plasma current is ramped down at a slow rate for a safe plasma termination.

In our simulation, the average electron density is assumed to be linearly ramped up and down along the total plasma current [8], although there is concern about the fuelling and pumping capability in ITER. The onset of a radiative collapse during the

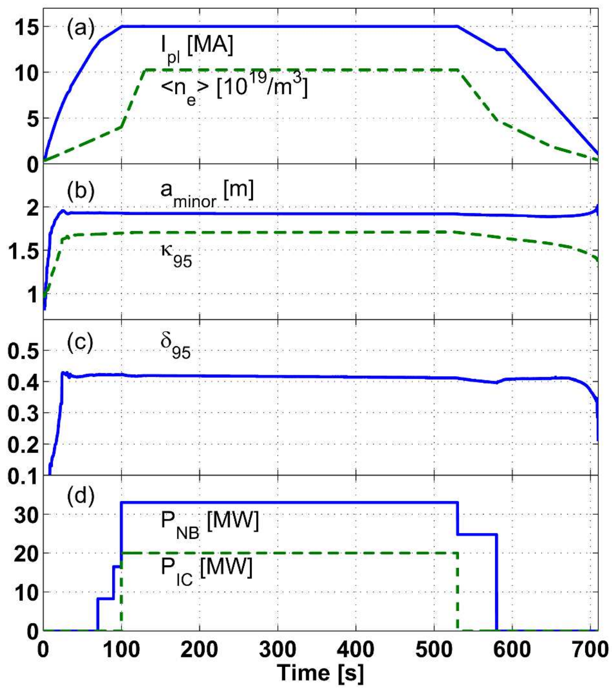

FIG. 2. ITER 15MA H-mode operation scenario. (a) The total plasma current, average electron density, (b) minor radius, plasma elongation, (c) plasma triangularity and (d) auxiliary H&CD powers are shown. Reprinted from Figure 2 of [5].

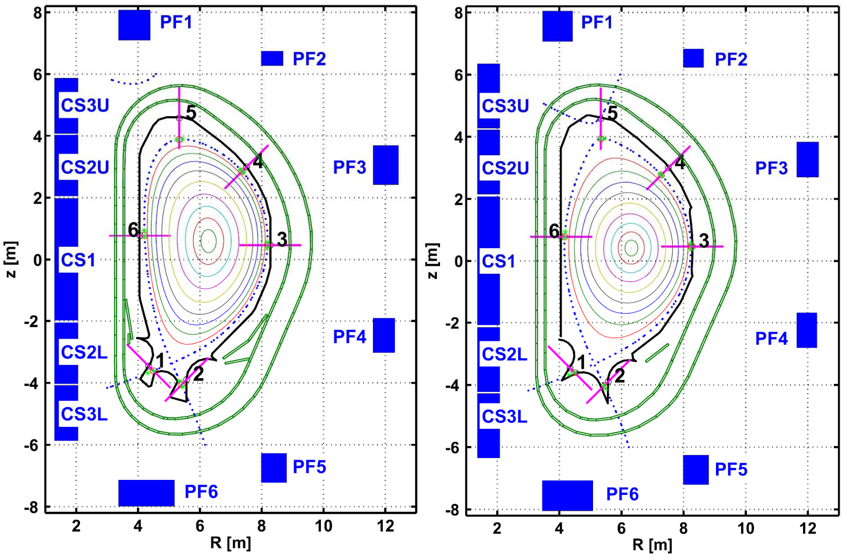

FIG. 3. Electromagnetic definitions of ITER for simulating the 15MA H-mode (left, [7], Reprinted from Figure 3 of [5]) and 12MA hybrid mode (right, [11]) scenarios. The PF coils (blue closed squares), vacuum vessel shells (green open squares), limiters (thick black lines), separatrix (blue dotted lines), six gap measurements between the plasma boundary and wall (violet lines with numbers) are shown.

termination of the plasma pulse is avoided by imposing the average electron density by trial. Ion and impurity density profiles are self-consistently calculated with an assumed flat effective charge profile. D-T (50:50) operation is assumed with the impurity species, He (3% of D), Be (respecting the assumed average effective charge), Ne (10% of Be).

In this simulation, the plasma started with a small bore (a_{minor}(t = 1.6s) = 0.8m) limited on the outboard side, and then it experienced a transition to a diverted single null configuration at about t = 29s. The plasma elongation was programmed to increase as the plasma column expands and to decrease during the plasma termination in order to avoid the onset of disruptive vertical displacement events (VDEs). 8.25MW of NBI was applied earlier starting from t = 70s, and then the power was stepped up to 16.5MW at t = 90s. This earlier application of the heating power during the current ramp-up was an obligatory choice to avoid the coil current limits by effectively reducing the resistive ohmic flux consumption and adding non-inductively driven current. 33MW of NBI and 20MW of ICRH power were used to trigger an L-H confinement mode transition and to maintain the plasma burn. Heat diffusivity profiles were calculated using the KIAUTO transport model [9] which controls the plasma energy confinement and mode transition respecting the global energy confinement time scaling laws [10]. The thermal collapse and plasma current redistribution were synchronized between the two codes to model effective sawtooth crashes. ELMs were not modelled.

A toroidally axi-symmetric plasma surrounded by limiters, passive stabilisers, vacuum vessel shells and PF coils is assumed as shown in the left figure in FIG. 3. The ITER plasma control system originally developed to operate around 15MA total plasma current has been modified to function with a varying plasma current [11], enabling its use for a full operation scenario including both the plasma current ramp-up and ramp-down. Standard ITER power supplies [12] are assumed. In the early phase of the plasma current ramp-up, a radial position controller was applied to stabilize the plasma boundary evolution. Both vertical and radial position controls were additionally weighted at low plasma current (0.4~7.5MA) to enhance the controllability. The radial position controller was switched to the plasma shape controller with a smooth transition after the plasma had a fully diverted configuration at around t = 29s.

Full tokamak discharge simulation results showed that the alpha particle self-heating power is slightly over 100MW and the fusion power ratio to the total auxiliary power, Q, is about 10 with 53MW of additional H&CD power during the current flat-top phase. The central safety factor value was quickly reduced at the beginning of the plasma current ramp-up, causing an early onset of sawtooth events. An L-H confinement mode transition was triggered when the main H&CD was applied at the start of flat-top phase. The vertical instability associated with a high internal inductance was controllable with the vertical position control system using the external PF coils. In this simulation, the evolution of the plasma boundary in a limited shape configuration was guided by the pre-programmed coil current and prescribed feed-forward voltage waveforms. After the plasma had a fully diverted configuration at about t = 29s, the shape controller started to control 6 gaps between the plasma and wall.

With the early application of NBI power, all the CS coil currents (see FIG. 4) were within the coil current limits [12] for all the operation, although the CS coils consumed a significant fraction of the volt–seconds for inductively driving the plasma current. The demand on the volt-seconds was significantly reduced during the flat-top phase, as the resistive ohmic flux loss decreased and non-inductively driven currents increased. However, the current in the PF2 coil briefly violated its limit around the end of the flat-top phase (EOF). However, this violation seems avoidable by either changing the plasma shape evolution or increasing the coil current limit itself, as addressed in the recent ITER design review [13]. The coil voltages were automatically within the coil voltage limits [12], since they were imposed in the control system as power supply voltage saturation limits. The consumption of the poloidal flux provided by the PF coil system was slightly less than the estimated one in the reference operation scenario. The imbalance current flowing in the vertical stabilization converter (VSC) and the total active power provided by the power supply system were well within the operational limits [12]. However, the electromagnetic forces on the CS and PF coils have not yet been evaluated in this study.

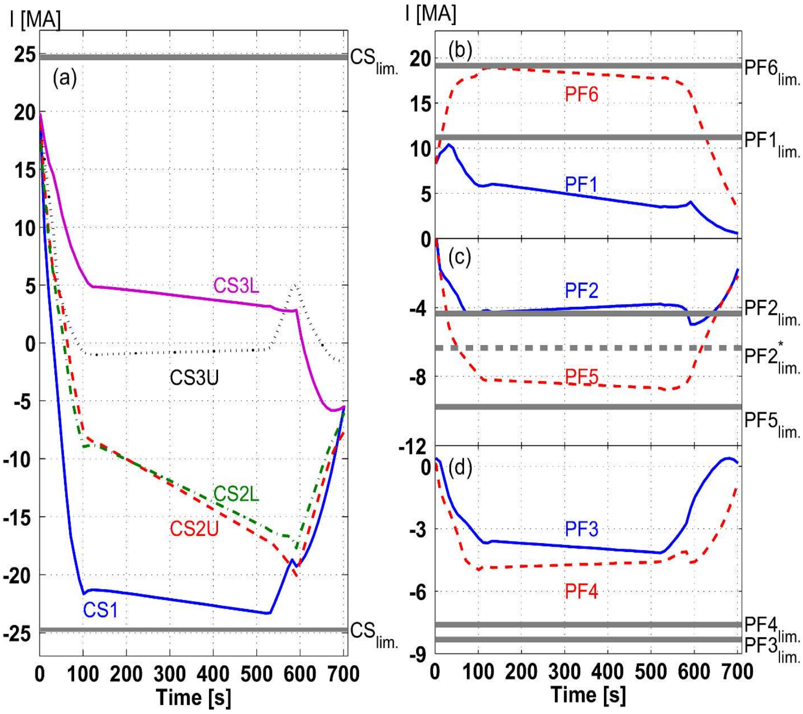

FIG. 4. Time traces of PF coil currents. The coil current limits are shown as thick grey lines. The PF2 coil current violated its limit ($PF2_{lim.}$) around the end of the flat-top phase. However, in the recent ITER design review [13], this coil current limit has been increased in absolute value (($PF2^*_{lim.}$). Reprinted from Figure 5 of [5].

3. LH Assisted Plasma Current Ramp-up

The capacity of LHH&CD for saving the poloidal flux consumed to produce the plasma current and for increasing the safety margins in operating the superconducting PF coils has been studied [6].

In this study, we have used a plasma current ramp-up scenario similar to the one presented in Section 2. The total plasma current is again assumed to be ramped up to 15MA within 100s. The average electron density is assumed to linearly increase. Anomalous electron and ion heat diffusivity profiles are prescribed by using a shaping function, $f = 1 + 6\rho^2_{tor} + 80\rho^{20}_{tor}$ [14-15] where ρ_{tor} is the square root of the normalised toroidal flux, and normalized in the KIAUTO transport model respecting the IPB98(y,2) H-mode scaling multiplied by a correction factor $H_{98} = 0.5$. An updated ITER electro-magnetic machine description [12] has been used (see the right figure in FIG. 3). In this simulation, the plasma started with a large bore (a_{minor}(t = 1.55s) = 1.6m) limited on the outboard side, and experienced a transition to a diverted SNL configuration at about t = 20s.

The effect of LH application on the current ramp-up in ITER has been studied using three variants of LH, a fully inductive current ramp-up, an early application of LH before the shape transition and a late application of LH after the shape transition. In the early/late LH application scenario, the LH power started at t = 8s/t = 32s and was progressively ramped up to its maximum value of 20MW over about 30s. However, the early application of LH gave a significant modification to the evolution of the plasma shape. Either redesigning the reference coil current waveforms or adding additional shape controls, such as an elongation control, was requested to provide an appropriate guidance for desired plasma shape transition. We have used the latter option in our simulation study. Heat deposition and LH driven current profiles were calculated by a toroidal ray-tracing/Fokker Planck code, DELPHINE [16].

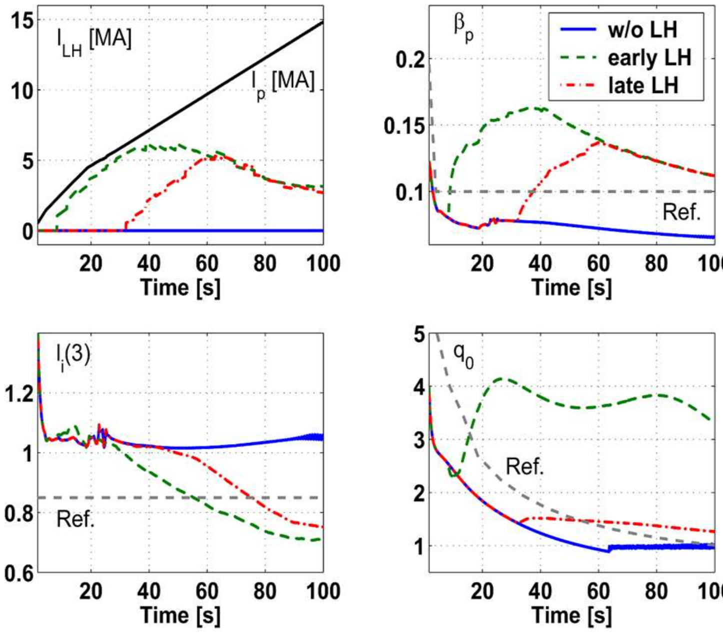

FIG. 5. Time traces of LH driven currents, poloidal plasma betas, internal inductances and central safety factor values. Three cases, without/early/late LH, are compared. Reprinted from the Figure 2 of [6].

The early application of LH provided a large fraction of the plasma current until the LH power reached its maximum at about t = 38s (see FIG. 5), whereas the fraction of LH driven current from the late application of LH was much smaller, because the total plasma current has already reached a higher value. The LH driven current then decreased as the plasma density increased further. The LH deposition and driven currents became very similar in both early and late application cases, once the same LH power level was reached at about t = 60s. The off-axis current driven by the LH application effectively reduced the plasma internal inductance. With the early/late LH application, it was reduced down to 0.71/0.75 at the end of the current ramp-up. The early LH application produced a negative or very low magnetic shear at the plasma centre, while the late LH application maintained q_0 above 1, barely avoiding the sawtooth instability.

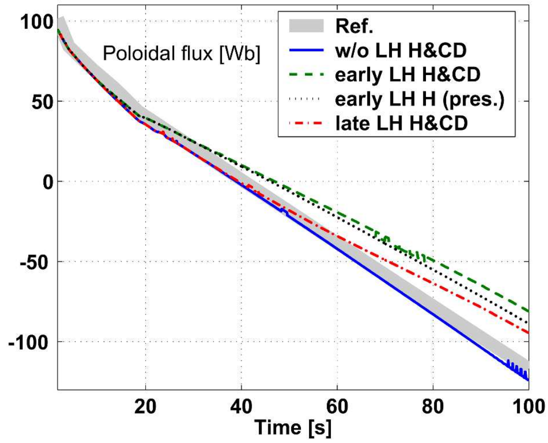

FIG. 6. Time traces of poloidal fluxes. Four cases, without LH H&CD, early LH H&CD, early LH H (heating profiles are obtained from early LH H&CD case, and then prescribed) and late LH H&CD are compared. Reprinted from Figure 5 of [6].

The evolution of the poloidal flux during the current ramp-up is compared for the three variants of LH application (see FIG. 6). With the early application of LH, about 43Wb of the poloidal flux (from -124 to -81Wb) was saved with respect to the ohmic ramp-up case. This amount is equivalent to about 500s of additional burn duration, if the same flux consumption rate assumed in the ITER reference scenario is applied. The contribution of the plasma heating and the non-inductive current drive to the poloidal flux saving has been investigated by performing an additional simulation with only LH heating profiles obtained from the previous early LH simulation (see black dotted line in FIG. 6). The increase of the plasma conductivity resulting from LH heating is mostly responsible for reducing the poloidal flux consumption (about 35.5Wb).

At the end of the plasma current ramp-up, in which LH was not applied, vertical oscillations of the plasma position were observed (see FIG. 7). These vertical oscillations grew until the position control was lost. When the plasma elongation was reduced by modifying the reference Gap5 (see inset in FIG. 7), the oscillations were significantly reduced. The application of LH added to the modification of Gap5 (red dashed–dotted line in FIG. 7) completely removed the vertical oscillations, presumably due to a slight reduction of li.

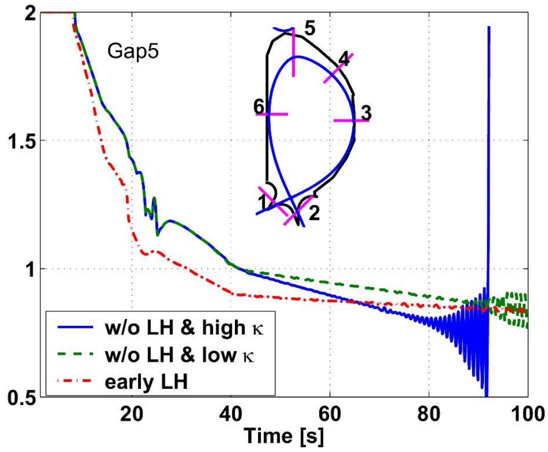

FIG. 7. Time traces of Gap 5 measured from the top of the vacuum vessel (see the nested small figure). Reprinted from figure 8 of [6].

4. ITER Hybrid Mode Operation

We have studied ITER hybrid mode operation, focusing on the operational capability of obtaining a stationary flat safety factor profile at the start of flat-top phase and sustaining it as long as possible by combining various non-inductively driven current sources [5].

A plasma current ramp-up scenario for ITER hybrid mode operation was generated by tailoring the 15MA H-mode ITER operation scenario presented in Section 3. The updated electro-magnetic machine description of ITER has been used, as shown in the right figure in FIG. 3. The plasma is assumed to start again with a large bore and to experiences a transition to a diverted SNL configuration at about t = 20s. The total plasma current is assumed to be ramped only up to 12MA at t = 77s and the average electron density at the start of plasma burn (SOB) is assumed to be $8.5\times10^{19}\mathrm{m}^{-3}$, to provide enough poloidal flux for a long pulse operation. The pedestal top is assumed to be at ρ_{tor} = 0.95 and the electron density at the separatrix is assumed to be 35% of the central value. 33MW of NBI (off-axis) and 20MW of ICRH (on-axis) are proposed to trigger an L–H mode transition and to initiate the plasma burn at the beginning of the flat-top phase. A confinement enhancement factor for the H-mode scaling, H_{98} = 1.2, is assumed in the KIAUTO transport model, to take into account the confinement improvement observed in the experiments targeting hybrid mode operation [17-19]. These are the assumptions used for standard simulation of ITER hybrid mode operation (‘Ref. sim.’).

To estimate the achievable range of plasma parameters in the ITER hybrid mode operation, we have conducted various simulations with slightly different assumptions on the energy confinement, heat conductivity profile shape and pedestal parameters. Firstly, a wider and higher pedestal was applied, assuming the pedestal top at ρ_{tor} = 0.92 and about twice the stored energy of the reference pedestal (‘Pedestal’). Secondly, the heat conductivity profile was imposed with a shaping function, $f(\rho_{tor}) = 1 + 3\rho^2_{tor}$, to produce a more peaked temperature profile (‘Peaked’). Thirdly, H_{98}=1.0 was assumed to examine the case in which the plasma stays in a standard ELMy H-mode confinement ('Low conf.'). Fourthly, purely gyro-Bohm global energy confinement scaling law proposed by McDonald [20] was applied without the multiplication factor which enhances the H-mode confinement. In this case, the wider and higher pedestal was again assumed to generate an acceptable electron temperature at the centre and pedestal ('DS03'). Lastly, 20MW of EC (slightly off-axis) or/and 20MW of LH (far off-axis) are added to the reference H&CD scheme, starting from t = 110s ('EC', 'LH' and 'EC&LH').

TABLE I: PLASMA PARAMETERS ACHIEVED IN VARIOUS ITER HYBRID MODE SIMULATIONS AT t = 200s. REPRINTED FROM TABLE 2 OF [5].

	Ref. sim.	Pedest.	Peaked	Low conf.	DS03	EC	LH	EC&LH
W_{th} (MJ)	291	286	287	220	369	312	314	330
H_{98}	1.18	1.19	1.17	0.97	1.39	1.20	1.20	1.20
β_N	2.07	2.03	2.05	1.56	2.62	2.21	2.22	2.33
$l_i(3)$	0.76	0.68	0.82	0.82	0.66	0.75	0.70	0.70
q(0)	0.94	0.90	1.00	0.96	1.25	1.31	0.96	1.23
$T_e(0)$ (keV)	25.5	21.5	28.6	20.1	30.4	30.3	27.3	31.2
$T_i(0)$ (keV)	23.8	20.0	26.5	19.0	27.9	23.5	25.3	25.1
$T_{e,ped}$ (keV)	3.14	5.48	3.14	2.34	4.87	3.41	3.46	3.66
$\rho_{tor,ped}$	0.95	0.92	0.95	0.95	0.92	0.95	0.95	0.95
I_{BS} (MA)	3.44	3.51	3.37	2.51	4.65	3.79	3.84	4.10
I_{NB} (MA)	0.71	0.66	0.83	0.46	0.99	0.65	0.67	0.67
I_{EC}/I_{LH} (MA)	-	-	-	-	-	0.41/-	-/0.89	0.33/0.94
P_α (MW)	71.9	65.4	72.1	41.8	109.7	76.3	82.1	84.7
Q	6.75	6.19	6.79	3.92	10.27	4.98	5.61	4.55

The simulation results are summarized in TABLE I. The standard hybrid mode simulation appears to be in the middle of parameter space bounded by either conservative [21] or optimistic plasma confinement assumptions. Application of the slightly off-axis EC driven current was effective in modifying the central q value, while the far off-axis LHCD had a small and delayed influence on the central q profile (see FIG. 8). Although the contribution of the far-off axis LHCD over a long time-scale has not yet been studied, it appears that the far off-axis LHCD is less effective for active control of q profile during the flat-top phase, in which the plasma current is high (it was very effective during the plasma current ramp-up phase. see Section 3). The application of

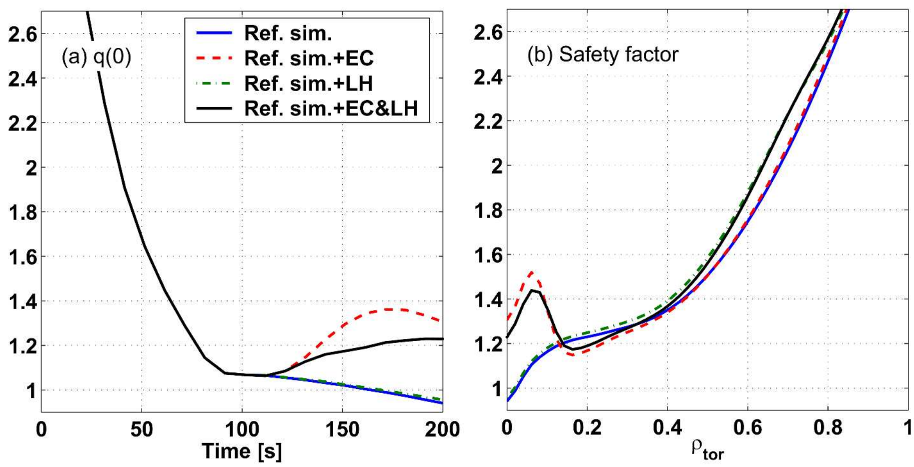

FIG. 8. (a) Time traces of central safety factors and (b) safety factor profiles at t=200s. Four cases, standard simulation, with additional 20MW of EC, with additional 20MW of LH and with both additional 20MW of EC and 20LW of LH. Repretined from figure 16 of [5]

ECCD was effective in modifying the central q profile, however the resulting profile was not flat at the centre. Application of an off-axis current located near the centre with a broad shape would be more promising for achieving a stationary flat q profile above 1.0.

In this study, a violation of the PF1 coil current limit was identified in the standard hybrid mode simulation after the plasma configuration was fully diverted at t = 20s. The PF1 coil current was increased above its upper limit due to the excessive reduction of volt-second consumption caused by the assumed confinement improvement. As an active method of avoiding this violation, modifying the evolution of the PF coil currents has shown its potential, although the vertical stability of the plasma is slightly deteriorated.

5. Conclusions

The combined DINA-CH/CRONOS tokamak discharge simulator has been successfully developed including all the major physics and engineering aspects. It has been used to study the feasibility of the proposed ITER operation scenarios and also to investigate several issues related to ITER operation. This simulator is now a fully mature platform with very strong potential for a full tokamak discharge simulation. This research experience is now a basis for developing a new free-boundary equilibrium evolution code, FREEBIE, which aims at providing a fully implicit data exchange scheme in coupling with CRONOS and at resolving limitations in improving the computational performance.

Acknowledgements

Part of this work, supported by the European Communities under the contracts of Association between EURATOM and both CEA and Confédération Suisse, and partly by the Fonds National Suisse de la Recherche Scientifique, was carried out within the framework of the European Fusion Development Agreement under the EFDA task, TW6-TPO-PLASMADYN. The views and opinions expressed herein do not necessarily reflect those of the European Commission

References

[1] Khayrutdinov R R and Lukash V E 1993 *Journal of Computational Physics* **109** 193
[2] Favez J-Y *et al* 2002 *Plasma Phys. and Cont. Fusion* **44** 171
[3] Artaud J-F *et al* 2010 *Nucl. Fusion* **50** 043001
[4] Kim S H *et al* 2008 *Proc. 35th EPS Conf. on Plasma Physics (Hersonissos)* vol 32D O-2.004
[5] Kim S H *et al* 2009 *Plasma Phys. and Cont. Fusion* **51** 105007
[6] Kim S H *et al* 2009 *Plasma Phys. and Cont. Fusion* **51** 065020
[7] ITER Technical Basis 2002 *ITER EDA Documentation Series No 24* (Vienna:IAEA)
[8] Lukash V E *et al* 2005 *Plasma Devices Oper.* **13** 143
[9] Artaud J F *et al* 2005 *Proc. 32nd EPS Conf. on Plasma Physics (Tarragona)* vol 29C P-1.035
[10] ITER Physics Basis 1999 *Nucl. Fusion* **39** 2204–2206
[11] Kim S H *et al* 2007 *Proc. 34th EPS Conf. on Plasma Physics (Warsaw)* vol 31F P-5.142
[12] Gribov Y 2006, *ITER D 247JZD* private communication
[13] Gribov Y 2008, *ITER D 2ACJT3* private communication
[14] Hogeweij G M D *et al* 2008 *Proc. 35th EPS Conf. on Plasma Physics (Hersonissos)* vol 32D P-5.034
[15] Parail V *et al* 2009 *Nucl. Fusion* **49** 075030
[16] Imbeaux F and Peysson Y 2005 *Plasma Phys. Control. Fusion* **47** 2041
[17] Joffrin E *et al* 2005 *Nucl. Fusion* **45** 626
[18] Staebler A *et al* 2005 *Nucl. Fusion* **45** 617
[19] Luce T C *et al* 2003 *Nucl. Fusion* **43** 321
[20] McDonald *et al* 2004 *Plasma Phys. Control. Fusion* **46** A215
[21] Sugihara M *et al* 2000 *Nucl. Fusion* **40** 1743